International Journal of Engineering Research & Technology (IJERT)
ISSN: 2278-0181
Vol. 3 Issue 10, October- 2014

A Novel Buckling Indicator using the Correlation Between in-Plane and out-of-Plane Displacements

N. A. Zanjani
A. Dervaric
S. Kalyanasundaram
Research School of Engineering
The Australian National University
North Road, Canberra 2601, Australia

***Abstract*— The current article investigates the buckling phenomenon in Aluminium sheets possessing different aspect ratios through a modified Yoshida buckling test. Specimens were uniaxially extended until catastrophic failure. Results of the optical photogrammetry technique revealed the evolution of out-of-plane displacements and in-plane state of strain in specimens during different stages of deformation. A Wrinkling Limit Diagram (WLD) was constructed based on induced principal strains in specimens. It was demonstrated that a specific WLD capable of differentiating between wrinkled and unwrinkled regions does not exist. Based on the cross sectional evolution of the specimen, a novel measure was proposed, showing to be a far more effective indicator of the wrinkling onset. Then, its applicability to some typical forming problems was studied.**

Keywords*— *Modified Yoshida Buckling Test, Principal strains, Wrinkling behavior, Wrinkling Limit Diagram.

I. INTRODUCTION

Wrinkling is a common type of instability during sheet metal forming. It manifests itself as low amplitude, small wavelength waves presented in different regions of the formed part. Underlying source of wrinkling is an increasing compressive stress experienced mostly in unsupported regions during a die forming practice such as sidewalls or flange areas. During a typical stamp forming process, a sheet of material flows into the die and conforms to the punch geometry, causing a reduction in the perimeter of the specimen proportional to its radial displacement. The induced deformations cause significant compressive stresses, triggering onset of instabilities such as local buckling (Wrinkling). Wrinkling is undesirable and deleterious as it affects the normal appearance of the final product, alters the required geometrical tolerances and degrades the mechanical properties of the component. Employing a stringent indicator for wrinkling assists manufacturers to discard the cumbersome trial-and-error procedure during die try-out, increasing manufacturing rate while reducing associated costs and production scraps.

One of the earliest attempts aimed at determination of wrinkling in sheet metals was performed by Senior [1]. In this article, a theoretical measure was proposed to predict the onset of wrinkling and to quantify the number of wrinkles observed in the flange area. The analysis was based on the energy method, stress-strain curve of the material and the flange geometry to specify the critical conditions triggering wrinkling. Hill's early works on stability of solids [2] attempted at formulating the stability condition as a boundary-value problem. It was found that only under some predefined stress conditions, the governing differential equation offers a unique solution. However, if induced strains or deformations are large, the uniqueness of the solution could not be guaranteed. Matsui, Iwata and Mori [3] investigated initiation and development of buckling in a diagonally stretched square specimen. Afterwards, a Finite Element (FE) analysis was conducted, and final results were verified by experimental outcomes. A clear correlation between loading conditions and material properties on buckling initiation and development was found. Szacinski and Thomson [4] investigated the possibility of constructing an empirical Wrinkling Limit Diagram (WLD), although they suggested that a mathematically definable WLD does not exist. In this investigation, detection of wrinkles on the surface of the drawn-sink bowls was done via a laser beam method. Based on experimental results, it was concluded that no definite theoretical WLD can be established to provide a criterion for initiation of wrinkling. Li, Brazil and Chu [5] used an experimental set-up using two strain gauges at both sides of an Aluminium sheet subjected to a non-uniform tensile stress field in a Yoshida Buckling Test (YBT). The evolution of wrinkles height was monitored as a function of stresses and strains developed in the center of sheets. It was found out that plastic anisotropy has the smallest effect on the occurrence of bifurcation phenomenon. Finally, it was concluded that WLD is not a material characteristic, unlike a Forming Limit Diagram (FLD), and therefore cannot be established uniquely for a specific material, simply because it is dependent to other factors such as geometry of the part, thickness of sheets, stress-path and friction. Bayraktar, Isac and Arnold [6] conducted experimental investigations to determine a Buckling Limit Diagram (BLD), conceptually similar to a WLD, for an Interstitial Steel (IFS) through the YBT. Circular blanks having thicknesses varying from 0.7 mm to 1 mm were used in these tests. The heights of wrinkles were measured as a function of extension applied to the specimens. Based on the experimental outcomes, it was concluded that thickness of sheets and yield stress of the material are determinant factors in wrinkling initiation during deep drawing operations. Narayanasamy and Loganthan [7] investigated wrinkling limits of pure Aluminium sheets through drawing process. Three different Aluminum grades, each heat treated by four different methods, were drawn through conical and tractrix

dies by a flat-head punch. Different WLDs based on the incremental strain ratios, stress ratios, and effective stress and strain increments were constructed. Based on the experimental and analytical outcomes, it was concluded that a WLD based on stresses, rather than strains, could give a better measure to distinguish between safe and wrinkled areas. More recently, Schleich, Albiez, Papaioanu and Liewald [8] investigated wrinkling behavior of Aluminium sheet alloys through a modified YBT. Different geometries were employed to simulate wrinkling initiation and development through uniaxial extension experiments. It was demonstrated that the precise moment of buckling initiation in specimens cannot accurately predicted.

Considering the lack of a reliable and rigorous, yet straight forward and simple to implement measure to evaluate buckling/wrinkling initiation, the current study aims at elucidating the wrinkling behavior of a common Aluminium sheet alloy via a modified YBT experiment. Inspired by the research conducted in [8], it utilizes various geometries possessing different aspect ratios in an attempt to offer a new measure for predicting wrinkling initiation. This research aims at establishing a novel and reliable wrinkling/buckling indicator to be implemented in a numerical simulation for predicting the onset of bifurcation. This reduces manufacturing costs related to cumbersome trial-and-error procedures in producing flawless products.

II. EXPERIMENTAL PROCEDURE

A. *Materials and preparation of specimens*

The specimens having 1 mm thickness were made of 5005-H34 Aluminum alloy. The H34 indicates a low temperature heat treated Aluminum alloy, in which grain structures are stabilized and residual stresses due to cold rolling process are relieved. Therefore, the final material can be treated as a homogenous, isotropic continuum. The geometry and dimensions of specimens are represented in Fig. 1 and table (I), respectively. Each experiment was repeated three times to ensure consistency and repeatability of the procedure.

Aluminium sheets were cut by water jet method to guarantee desired accuracy and obtaining specimens free of any residual stress. All samples were annealed to obtain isotropic, highly ductile specimens. This prevented tearing of the samples before occurrence of any possible buckling during experiments. Isotropic property was also desirable to avoid any influence on wrinkling behavior due to different yield strengths in various material directions.

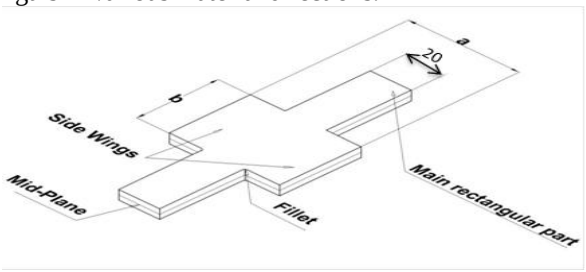

Fig. 1: Specimens' geometry

TABLE I. TABLE STYLES

Sample	a(mm)	b(mm)	Sample	a(mm)	b(mm)
4055	40	55	6055	60	55
4065	40	65	6065	60	65
4075	40	75	6075	60	75

Annealing was carried out in an electric muffle furnace by ramping up the temperature to 425° with a rate of 3 °/min. Afterwards, the specimens were kept in the furnace for two hours, followed by an unforced cooling process to ambient temperature during an 18-hour time span. Followed by cutting and annealing procedures, each specimen was deburred and cleaned with an acetone solution. The deburring process minimized the possibility of premature failure in samples. The surface cleansing was also done to remove any oil and dirt from the surface of the specimens, preparing it for subsequent painting procedure.

To achieve high quality surface painting required for strain measurements, specimens' surfaces were covered with an evenly distributed thin layer of a dim white coating as the primer. Then, a stochastic black dot pattern was applied on top of the primer. Fig. 2 represents a typical painted sample, prepared for experiment. After painting, samples were allowed to be dried completely, but were used within three hours after painting. This prevented excessive drying of the paint leading to flaking off from the surface during experiment, as a result of a reduction in paint's elasticity.

B. *Experimental equipment*

The principal equipment used to conduct buckling experiments included a universal testing machine and an optical measurement system. A hydraulically driven 8874 INSTRON machine was used to extend and to trigger out-of-plane displacements in specimens at some stage of experiment. A 3D photogrammetric system (ARAMIS) was also employed to measure displacements and to calculate strains on the surface of specimens during deformation. The ARAMIS system is a non-contact deformation measurement system, utilizing two high speed CCD cameras (stereo-type), capable of computing 3D strains on the surface of specimens via a Digital Image Correlation (DIC) technique. Prior to conducting any strain measurement, the cameras was positioned in place and then calibrated, using a proper combination of relative distances, angles and lenses, to satisfy the required measuring volume for each individual experiment.

Fig. 2: Painted surface of a specimen

The calibration procedure guaranteed an accurate deformation measurement, essential to calculate strains precisely by applying a deformation gradient tensor. This was done automatically by the built-in algorithm installed on the ARAMIS. The accuracy of the ARAMIS system was 0.005% of calculated strains.

C. *Experimental set-up*

The configuration of INSTRON and ARAMIS systems employed in this study is shown in Fig. 3. Two CCD cameras are mounted on a tripod facing toward the painted surface of the specimen. A 500 Watt light source was placed behind cameras to provide required illumination. Specimens were initially fixed by lower grippers of INSTRON, followed by a snap-shot taken by the ARAMIS to indicate the strain-free condition in samples. Afterwards, upper grippers were closed to clamp specimens. Another image was taken by the ARAMIS, specifying deformations introduced in specimens by closing upper grippers.

Finally, the specimens were uniaxially extended up to the failure, while strains and their evolution were calculated by the ARAMIS system. To obtain required precision, the cross head speed of INSTRON and the ARAMIS sampling rate was set to 10 mm/min and 1 Hz, respectively. This resulted in recording an image of the deforming specimen in every 1/6 mm extension. Out-of-plane deformations during uniaxial extension were also recorded by the ARAMIS to elucidate buckling onset.

III. THEORETICAL DESCRIPTIONS

A. *Pearson's Correlation Coefficient (PCC)*

The Pearson's product-moment Correlation Coefficient, or simply Correlation Coefficient (PCC) introduced by symbol r, is a measure of linear dependency between two variables. In the context of the current study, this factor is adopted to establish an effective measure indicating the linearity of a transverse section on the specimen to the out-of-plane displacements, and therefore to determine the onset of buckling. This factor could be expressed by (1).

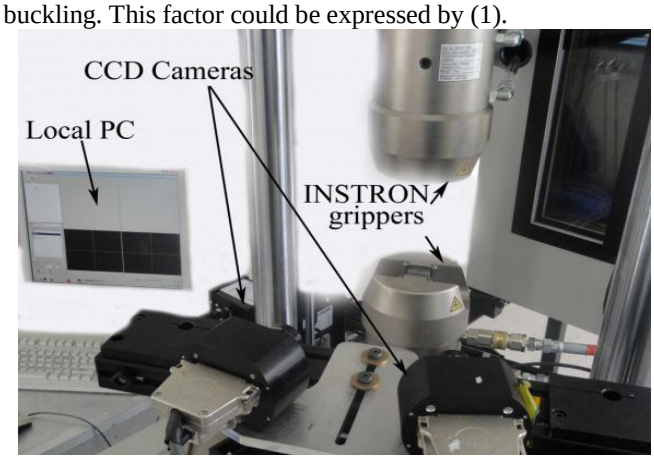

Fig 3: Experimental set-up

$$r = \frac{\sum_{i=1}^{n}\left(\left(x_i - \bar{x}\right)\left(z_i - \bar{z}\right)\right)}{\sqrt{\sum_{i=1}^{n}\left(x_i - \bar{x}\right)^2 \sum_{i=1}^{n}\left(\left(z_i - \bar{z}\right)^2\right)}} \qquad (1)$$

Where (x,z) are variables under examination , and $(\bar{x},\bar{z})$ introduce their average values. The PCC indicates the strength of a linear relationship between x and z variables, fluctuating between -1 and +1. PCC equal to -1 or +1 indicates a complete linear dependence between the two variables. Negative values of PCC exhibit an inverse dependency between the two variables. If PCC becomes zero, then two variables do not have any dependency to each other. Presence of any random noise in data decreases the magnitude of PCC away from ideal. Another important property of PCC is its invariance to linear transformations. This guarantees the current measure is not affected by the conversion of measurement units. In the current study, the parameter (x) refers to a location on the surface of the specimen (one of its in-plane coordinates) and parameter (z) indicates the out-of-plane displacement of that point.

IV. RESULTS AND DISCUSSIONS

A. *Initiation of out-of-plane displacements*

Initially, specimens were fixed between grippers of INSTRON. Friction between grippers' jaws and specimens induced compressive stresses, resulting in an early onset of buckling. This was caused by the low bending rigidity of samples, possessing small cross sections. The contour of a transverse section before and after clamping is shown in Fig. 4. This Fig. indicates 0.06mm difference between z coordinates at different locations caused by grippers' effect. However, as the experiment progressed, the out-of-plane displacements started to decrease instantaneously due to counteracting effect of uniaxial stretch (Fig. 5). This Fig. shows an initial out-of-plane displacement at the mid-point (intersection of two symmetry axes) of a typical specimen occurring around 0.5 s, followed up by a sudden increase up to 0.45 mm. Two factors contributed to the evolution of out-of-plane deformations: Gripper's effect and high sensitivity of ARAMIS to small changes in strains caused by environmental effects. After specimen was completely clamped within grippers' jaws, it took 6 to 8 seconds to actuate the INSTRON machine, during which the specimen was heated-up by the light source. The generated heat increased out-of-plane displacement in the specimen due to compressive stresses, resulting from applied boundary conditions. Initiation of uniaxial extension around 8s decreased the z displacement of the mid-point to around 0.1 mm at the end of the experiment.

It is noteworthy to mention that induced out-of-plane displacements in specimens were difficult to detect by naked eyes. However, highly sensitive ARAMIS system was able to capture out-of-plane displacements in most specimens. This is evident from the curvature of the transverse section on a typical specimen after onset of out-of-plane deformations as depicted in Fig. 6. The deformed shape of the mid-plane section undoubtedly confirms initiation of buckling (A bifurcation from in-plane to out-of-plane displacements).

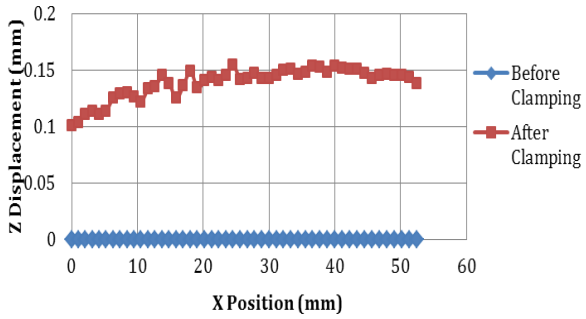

Fig. 4: Shape of a specimen's mid-section before and after clamping

The change in mid-plane geometry was the primary criterion used to determine the onset of buckling for establishing a Wrinkling Limit Diagram (WLD). The authenticity of this prediction will be verified by a more rigorous measure of buckling presented in section 4.3.

B. Construction of a Wrinkling Limit Diagram (WLD)

A specimen subjected to external loadings experiences different deformation modes in different regions. The induced deformation modes, however, evolves during forming due to the change of stress (strain) state in the specimen. Different deformation modes experienced during a typical forming process are shown in Fig. 7. Induced deformations are specified by the ratio of minor to major strains, known as Strain Ratio (SR). In that sense, each mode of deformation could be characterized by a unique strain ratio, as follows:

SR =	+1	Biaxial Stretch
SR =	0	Plane Strain
SR =	- 0.5	Uniaxial Stretch
SR =	-1	Shear Mode
SR =	- 2	Wrinkling

Specifying induced principal strains determines induced deformation modes in a specimen. To specify onset of wrinkling in industrial practices, it is common to utilize strain ratio as an indicator. The induced strain ratios at the last stage of deformation prior to onset of buckling are employed to construct a WLD.

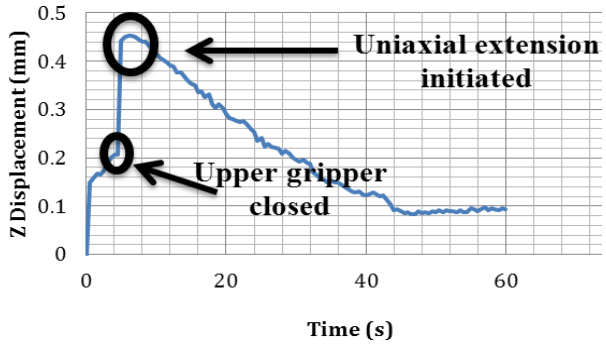

Fig. 5: Z-displacement evolution at the mid-point of a typical specimen

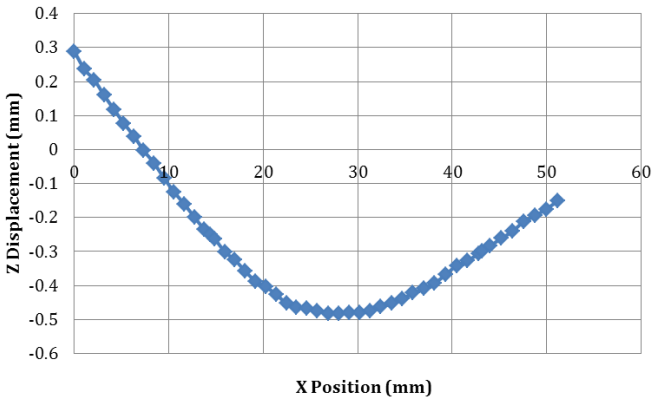

Fig. 6: Induced curvature in the mid-section of 4055A specimen

The WLD is a graphical representation of major versus minor strains induced in a specimen at the onset of wrinkling, differentiating between un-buckled and buckled states of the material. Pre-assumptions in applicability of such a diagram include:

- Wrinkling tendency is an inherent material characteristic; therefore it is not affected by the specimen dimension and geometry
- Wrinkling could only be determined by the surface strains of a specimen, and it is not affected by through-the-thickness strains

To verify the validity of these assumptions, the YBT was conducted on Aluminium specimens with different aspect ratios. The outcomes of these experiments are investigated in following sections to examine the validity and applicability of WLD in determination of wrinkling onset and to verify the necessity of establishing a more reliable indicator on wrinkling.

C. Evolution of WLD in 4065 specimens

Figs. 8-10 depict minor and major strains on the surface of a typical specimen (4065) at different stages of uniaxial experiment. As discussed previously in section 4.1, the initiation of wrinkling in this specimen was validated by the shape of its mid-plane section taken out from ARAMIS. The curvy shape of mid-section determines initiation of out-of-plane displacements during in-plane loading of the sample.

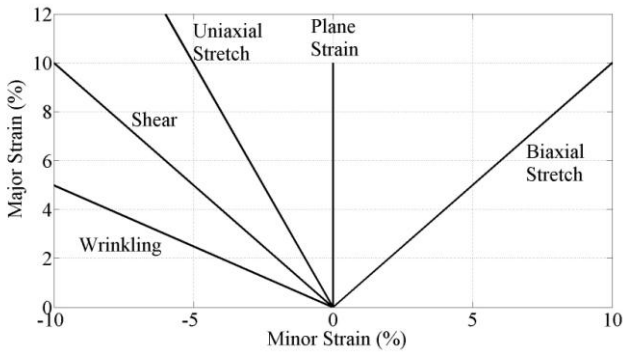

Fig. 7: Induced different deformation modes specified in strain space

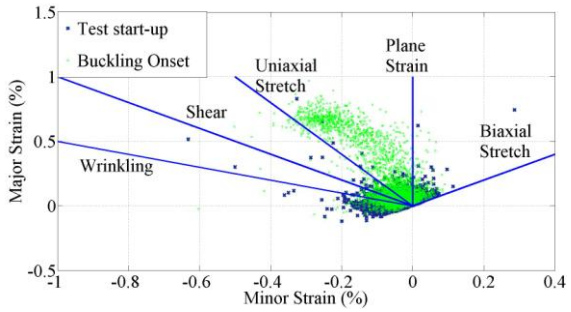

Fig. 8: Principal strains distributions at the start-up of the experiment and onset of buckling

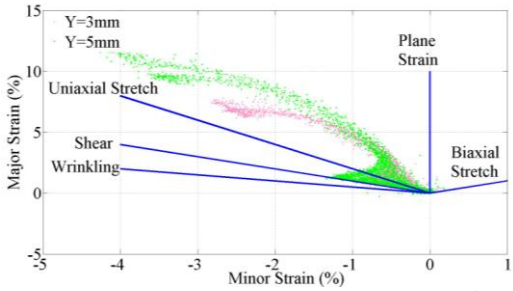

Fig. 9: Principal strains distributions at 3mm and 5mm of extension

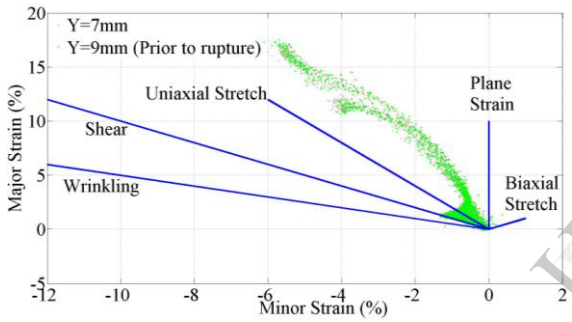

Fig. 10: Principal strains distributions at 7mm and 9mm of extension

In Fig. 8, the distribution of principal strains is depicted at two stages: Start of experiment when grippers were closed and at the onset of buckling. Figs. 9 and 10 depict the principal strains evolutions at 3mm-5mm and 7mm-9mm extensions, respectively. It is obvious that out-of-plane deformation in this specimen has commenced at very early stages of extension. Distribution of principal strains in Fig. 8 demonstrates accumulation of data points around the origin of strain space. A minority of these data points exceed the commonly assumed wrinkling limit, while majority of them are located around uniaxial extension and plane strain modes. This percentage drops significantly once specimen started to buckle out. This behavior is more evident at higher extensions as depicted in Figs. 9 and 10. In fact, the more the specimen was extended, the more its WLD diverged from the known wrinkling limit (SR=-2), tending toward other deformation modes. This is in complete contrast to what is expected to be observed in the WLD of a specimen exhibiting wrinkling: The more the specimen wrinkles out, the more data points should be located under WLD. These results clearly demonstrate the inadequacy of a WLD in determination of wrinkling onset and its evolution merely by just two components of strain vector, e.g. major and minor strains.

D. Correlation Coefficient as a buckling/wrinkling indicator

A transverse section passing through the mid-point of the specimen was originally a straight line prior to the extension. During the experiment, this section maintained its shape until onset of buckling. Initiation of buckling, being considered as a bending condition, transformed the shape of the straight line to a curved one, as specified in Figs. 4 and 6. Direct observation of this profile during the experiment is not neither a scientifically rigorous approach nor an accurate method to predict onset of buckling. It requires measurement of out-of-plane displacements which is very subjective and hard to recognize. This method can misguide the observer due to initial uneven surface of the specimen. Finally, during real production practices, studying the probability of wrinkling initiation and the early detection of wrinkling via this method is very difficult, if not impossible.

Introduction of an objective metric to measure the degree of curvature would be necessary. This could be an analytical measure to be employed in a numerical simulation or to be applied during experimental evaluation by a system similar to the current optical measurement device. In this study, the PCC parameter appears to be a suitable candidate as it can be employed as a measure of the linearity between two different displacements. Any given section passing through the surface of the sample at two different stages only differ in the presence of the out-of-plane displacements, causing a change in the magnitude of calculated PCC. The change in the magnitude of PCC can be evaluated as a proper measure for the onset of buckling as it considers the evolution of the buckling parameter over a selected surface area (or a section) rather than on a localized point.

Prior to the onset of buckling, the absolute value of PCC on the transverse section is approximately equal to one (±1). After buckling starts, this coefficient changes abruptly due to a sudden change in the shape of the section from a straight to a curved one. Therefore, this possibly could be employed as a metric to indicate buckling initiation, as described later in the evolution of PCC in different specimens.

A closer view of evolution of PCC in 4055 A&B specimens with 1mm thickness are presented in Fig. 11 and 12, respectively. It could be clearly observed that buckling of the specimens A & B started at 1.5s and 2.5s, respectively. It is also evident that initial variation in PCC prior to 1s is not related to onset of buckling, rather caused by state of the specimen prior to clamping. Onset of buckling in these two specimens is evident through the abrupt change of PCC and its continuously increasing trend.

Evolutions of PCC in two other specimens are shown in Figs. 13 and 14. Although both 4065 samples exhibited onset of buckling, sample (B) showed an initially rapid change, while PCC of sample (A) decreased more gradually. One rational explanation could be the initial state of sample (A), demonstrating an initially non-planar condition. This could cause unpredictable effects on the deformation behavior of the sample. During heat treatment, specimens were propped up against the side walls of the furnace. The sustained elevated temperature inside the oven could cause undesirable deformations in the specimens under their own weight. Another possibility could be rapid onset of buckling prior to action of ARAMIS in taking the very first images.

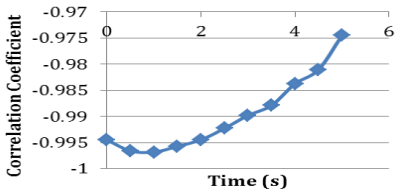

Fig. 11: Evolution of correlation coefficient for the 4055A-1mm specimen

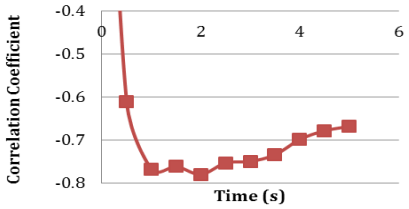

Fig. 12: Evolution of correlation coefficient for the 4055B-1mm specimen

To verify the validity of using PCC as an indicator of buckling behavior, the cross-section of two specimens at the last stage of deformation are depicted in Figs. 15 & 16. By observing the shape of transverse cross section, it could be decisively concluded that specimen 6075A didn't experience out-of-plane deformation, while 6075B sample buckled out. The PCC values calculated for these specimens, depicting the same results, shows the proposed indicator to be an accurate measure of the wrinkling onset. However there could be several possibilities associated with the different behavior of two seemingly identical specimens. Primarily, the annealing process may have introduced some initial distortion that differed between the specimens, causing this different buckling behavior. Another possibility could be due to different microscopic structure of the specimens, causing specimens start to buckle at different strain states, considering the fact that buckling is an imperfection driven phenomenon.

E. Special cases

In the current study, the application of the proposed measure in specifying the onset of buckling was examined during uniaxial extension of different Aluminium samples. However, there are some special cases needed to be addressed properly to elucidate the efficiency of the proposed criterion in any practical forming exercise and to propose required modifications to make this indicator more efficient. These cases include: (1) wrinkling phenomenon and (2) forming of an initially flat plate to a cylindrical shape. The underlying reason for the importance of wrinkling is its localized effect compared to buckling that affects the whole surface of specimen. Forming of a flat plate to a cylindrical shape is another case needs to be addressed properly as it contains out-of-plane bending conditions similar to what was observed during buckling of specimens in the current study.

Fig. 17 shows wrinkles on the surface of a shell during an arbitrary forming process. In-plane coordinates are depicted by x and y axes and out-of-plane displacements are specified by z coordinate. The anti-symmetric nature of a wrinkling problem, causes the induced normal displacements alternatively change between identical positive and negative values over the entire surface of specimen. This causes the calculated PCC to be equal to: r = ±1.

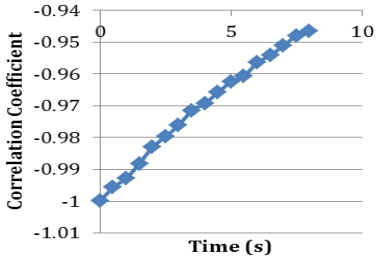

Fig. 13: Evolution of PCC for the 4065A-1mm specimen

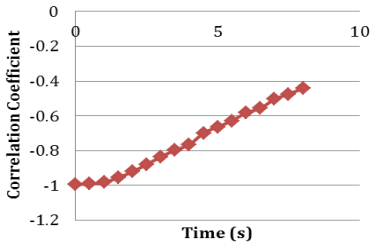

Fig. 14: Evolution of PCC for the 4065B-1mm specimen

This means that although the specimen has experienced wrinkling condition, the proposed criterion cannot detect it. This is due to the fundamental difference of wrinkling with the buckling phenomena studied here, as the former is signified by reciprocating small waves appeared on the surface of the specimen, while the latter causes the specimen to bend along with a very large curvature. To address this issue, the absolute values of the involved parameters should be incorporated to the original PCC equation. This converts (2) to the following:

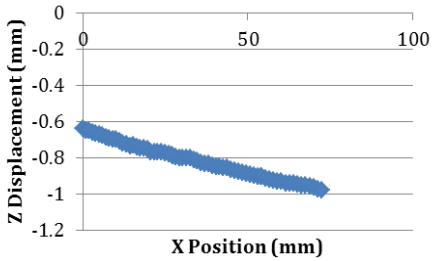

Fig. 15: Out-of-plane displacement through mid-transverse section of 6075A-1mm specimen prior to fracture

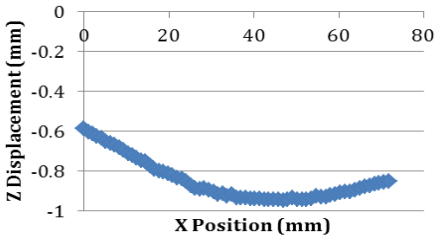

Fig. 16: Out-of-plane displacement through mid-transverse section of 6075B-1mm specimen prior to fracture

$$r = \frac{\sum_{i=1}^{n}\left(\left(x_i\right)\left(z_i\right)\right)}{\sqrt{\sum_{i=1}^{n}(x_i)^2 \sum_{i=1}^{n}(z_i)^2}} \qquad (2)$$

Employing (2) causes the counteracting effect of displacements toward negative direction of z axis to be eliminated. Equation (2) can be treated as the modified version of PCC specified as in (1), applicable to both buckling and wrinkling problems.

The second problem is regarding the forming of an initially flat plate to a final cylindrical profile, as depicted in Fig. 18. The in-plane coordinates are specified as (x) and (y), while (z) axis depicts out-of-plane displacements. If (1) is applied to find the relationship between (y) and (z) coordinates, the resultant r would be some values other than ±1, indicating the occurrence of compressive instabilities in the blank. This is due to the fact the shape of sections parallel to y axis is continuously changing, possessing continuously increasing z values. However, in reality no buckling or wrinkling has initiated. To address this problem, coordinate (y) should be substituted with coordinate (x) to obtain meaningful results. This yields constant r values of ±1, depicting un-buckled state in the specimen.

To address similar problem in any forming practice and to be able to accurately differentiate between homogenous forming conditions and localized compressive instabilities such as buckling or wrinkling, further verifications on the results of the proposed criterion should be conducted. Generally, due to the nature of the proposed wrinkling/buckling detector, the surface area under investigation should be changed accordingly to evaluate the possibility of wrinkling onset on different sections (areas). If the reported PCC on large areas coincides with the values reported for very small areas, then the detected phenomenon is probably a forming condition rather than localized buckling or wrinkling instabilities. In other words, the occurrence of any out-of-plane instability should be checked by the conformity of the results between different surface areas under investigation. Commonly, in a localized buckling or wrinkling phenomena, the instability initiates within a very small surface area and develops to larger surfaces.

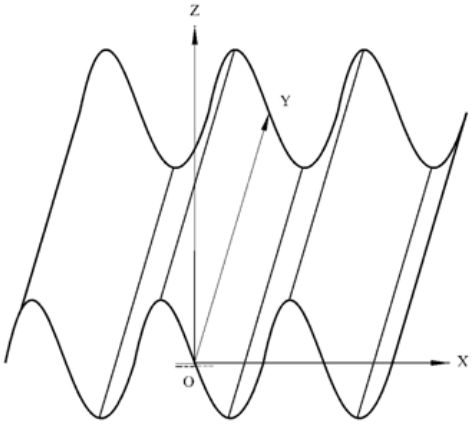

Fig. 17: Wrinkles on the surface of a thin sheet

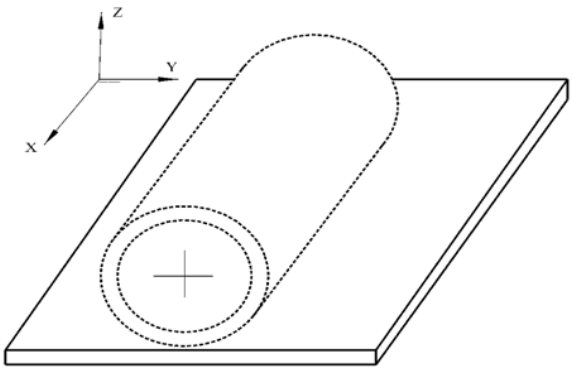

Fig. 18: Forming of a flat sheet to a cylindrical shape

However, in a forming practice, the out-of-plane displacements start instantaneously at a very large scale or probably on the whole surface of the specimen. Therefore, the application of the proposed criterion to detect early onset of local wrinkling/buckling seems to be efficient and applicable to practical forming exercises, as it can be effectively modified to consider initiation of these phenomenon over a very small regions on the sheets.

V. CONCLUSIONS

A series of experiments were designed to induce out-of-plane deformations in specimens made of a 5005 series Aluminium alloy. The evolution of transverse sections in specimens was used as a metric to determine the onset of buckling. Almost all specimens exhibited out-of-plane deformations during some stages of extension. It was shown that the commonly employed WLD could not accurately predict the onset of buckling in these specimens. It was observed that strain ratio of buckled regions is constantly moving away from the commonly known critical wrinkling limits after onset of bifurcation (SR= -2). It was elucidated that a unique WLD could not efficiently predict the wrinkling tendency of a material just based on the surface strains. This proved the necessity of employing a third parameter, rather than major and minor strains, in predicting wrinkling initiation in a material. Further investigations demonstrated the effectiveness of a newly introduced criterion in predicting buckling in specimens. This criterion was established based on the correlation between in-plane and out-of-plane deformations along an arbitrary section on the specimen. The correlation coefficient was applied on a transverse section of the sample passing through its mid-point. The onset of buckling was determined specifically by a noticeable and evident change in the magnitude of this correlation coefficient. This metric is superior to visual observations in different ways: First, using this technique improves the objectivity of the measurement. Second, it is superior to other techniques that specifically measure out-of-plane displacements on limited surface points, as it considers the average value of a variable over a surface area and during an extended time-span. Thirdly, by changing the surface area on which this criterion is applied, the possibility of wrinkling initiation can be re-evaluated and the precise location of wrinkling occurrence can be determined. Furthermore, this process enables the differentiation between a stochastic random instability observed on the surface of a specimen, such as wrinkling, and a homogenous deformation behavior, such as forming by

bending. Fourthly, the proposed indicator can be implemented directly into a numerical simulation, removing the necessity to measure induced out-of-plane displacements for the possibility of wrinkling in the formed parts.

REFERENCES

[1] Senior B. W., 1956. Flange wrinkling in deep drawing operations. Journal of mechanics and physics of solids. 4, 235-246.
[2] Hill R., 1958. A general theory of uniqueness and stability in elastic-plastic solids. Journal of mechanics and physics of solids. 6, 236-249.
[3] Matsui M., Iwata N., Mori n., 1987. Initiation and growth of buckling in the biaxial diagonal tensile test on steel sheet. Journal of mechanical working technology. 14, 283-294.
[4] Szacinski A. M., Thomson P. F., 1991. Investigation of the existence of a wrinkling-limit curve in plastically-deforming metal sheet. Journal of materials processing technology. 125-137.
[5] Li M., Brazil R. L., Chu E. W., 2000. Initiation and growth of wrinkling due to non-uniform tension in sheet metal forming. Journal of experimental mechanics. 40, 180-189.
[6] Bayraktar E., Isac N., Arnold G., 2005. Buckling limit diagrams (BLDs) of interstitial free steels (IFS): Comparison of experimental and finite element analysis. Journal of Materials Processing Technology, V.164-165, 1487–1494.
[7] Narayanasami R., Loganathan C. 2006. Study on wrinkling limit of a commercially pure sheet metals of different grades when drawn through conical and tritrix dies. Journal of materials science and technology. 419, 249-261.
[8] Schleich R., Albiez C., Papaioanu A., Liewald M., 2009. Investigation on simulation of buckling of Aluminium sheet alloys. 7th European LS-DYNA Conference, Salzburg.